Pulsed Bremsstrahlung Spectrum Measurement using a Fast Scintillator

Masakuni NARITA*
Yasutomo OZAWA*

(Received, July, 24, 1974)

Abstract

The energy spectrum of pulsed bremsstrahlung from a 4 MeV electron linac was measured using a plastic scintillator and an electric integral system. The measuring system, consisting of a 100 MHz discriminator, an integrator and a multichannel PHA for a scaler, works as a single channel pulse height analyzer which made it possible to separate multiple photons detected during a single linac pulse width. From the measured pulse height distributions, the spectrum of pulsed radiation source is deduced by the use of numerical unfolding techniques.

1. Introduction

A few attempts have been made to measure the bremsstrahlung energy spectra produced by pulsed electron beams from linear accelerators[1]. These measuring systems generally utilize techniques to reject such scintillation events in which more than one gamma ray is detected during a single linac pulse.

In this paper, a plastic scintillator NE 102A ($1.5'' \times 1''$) and the same system using the photon number frequency distribution measurements during a pulse width in our previous paper[2] were also used, in such a way that multiple photons detected can be separated during a single linac pulse width.

The photon energy spectra were determined from the pulse height distributions of the scintillator using the usual response matrix method. The response function of the scintillator was calculated from the Klein-Nishina formula in several MeV energy range. Another function, the rectanglar distribution extending from zero energy up to the Compton edge, was also used in the differential method.

The present method is superior to the others[6)~9)] for the pulsed radiation measurements in its capability of determining both the photon energy distribution and its frequency function using the same system.

2. Experimental System

As photon detector a plastic scintillator NE 102A ($1.5'' \times 1''$) with a photomultiplier tube (EMI 9594B) was used, which permitted resolution of nano-second

* Department of Nuclear Engineering, Faculty of Engineering, Hokkaido University, Sapporo, Japan.

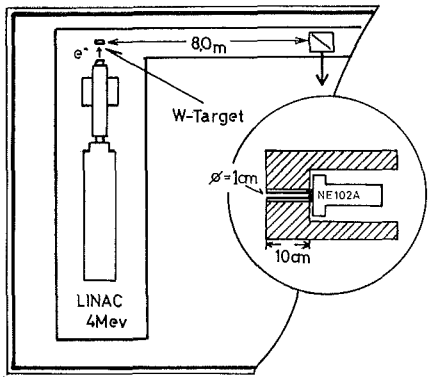

Fig. 1. Experimental arrangement

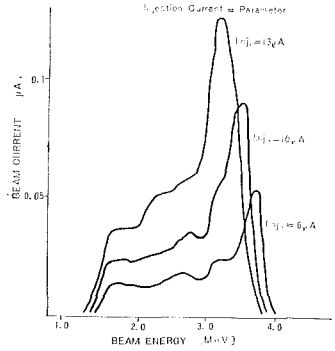

Fig. 2. Electron beam energy distribution used in this experiment

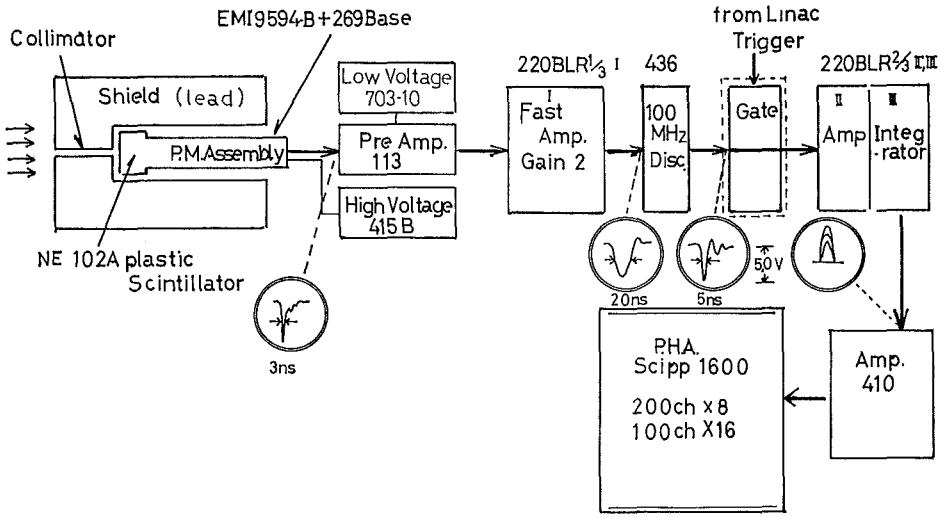

Fig. 3. Block diagram of the data acquisition system

photon single pulses. Lead shield and collimators were used to ensure that only the bremsstrahlung target area could be seen by the plastic scintillator. Figure 1 shows the experimental arrangement used for the linac photon beam measurement. The electron beam from 4 MeV accelerator was incident upon a 0.5 mm thick tungsten target. The linac operating parameters were 1.6 μsec electron beam pulses repeated at 100 pulses/sec, with an average beam current of about 2 μA. The beam energy distributions of the machine were measured with a magnetic spectrometer as shown in figure 2. Then the most probable energy is 3.8 MeV in this experiment. Figure 3 shows a block diagram of the data acquisition system. Electrical signal pulses at the photomultiplier anode with 2 μsec pulse width are fed to the 100 MHz discriminator through a preamplifier. This discriminator has trigger levels which can be used to select the pulse heights having energy information and generates an output pulse of a fixed amplitude of 5 V and 2 nano-second for each gamma rays interaction in the

detector that is separated by more than several nano-seconds.

The output signals of the discriminator pass through a gate in synchronization with linac triggers and are amplified with a pulse amplifier to readily cause signal pulses to change its pulse height at the following integrator. The integrator has a time constant of μsec, and thus the pulse out of the integrator is proportinal to the number of signal pulses detected during a pulse. Display on the pulse height analyzer for a selected trigger level shows pulse number discrete spectra in figure 4.

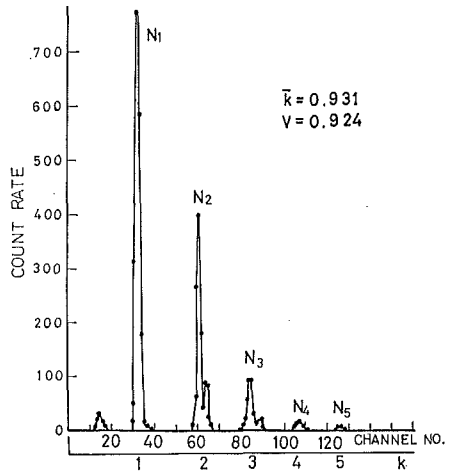

Fig. 4. Typical pulse frequency distribution during linac pulse width

3. Pulse Height Spectra

Figure 4, a typical frequency distribution, at a fixed discriminator level x, can be seen as several peaks corresponding to 1, 2, 3, $\cdots$ and k_m signal pulses per linac pulse respectively. Each peak shows the frequency $N_k(x)$ exactly counted k signal pulses per linac pulse during the observed time. From the distribution obtained, the number of signal pulses can be derived using formula.

$$N(x) = \sum_{k=1}^{k_m} kN_k(x) \qquad (1)$$

and the frequency of the occurrence of no signal pulses in the course of the observed time can be obtained by

$$N_0(x) = N_T - \sum_{k=1}^{k_m} N_k(x) \qquad (2)$$

where N_T is the number of the linac pulses generated during that time interval. The mean signal pulses per linac pulse width detected beyond the trigger level x is estimated from

$$\bar{k} = N_k(x)/N_T \qquad (3)$$

and the variance of them is

$$V(x) = \sum_{k=1}^{k_m} k^2 N_k(x)/N_T - (\bar{k}(x))^2 . \qquad (4)$$

A differential pulse height distribution $f(x_i)$ is obtained by

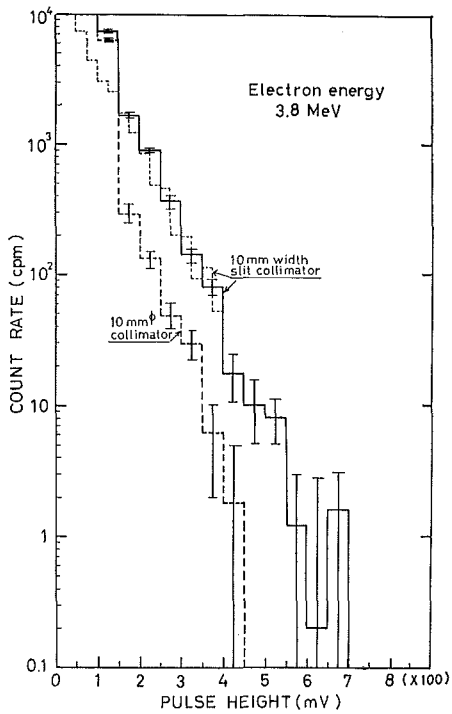

Fig. 5. Pulse height distribution measured at 3.8 MeV electron beams

$$f(x_i)=\bar{k}(x_{i+1})-\bar{k}(x_i), \qquad i=1, 2, \cdots i_{\max}, \tag{5}$$

and the variance is

$$V_d(x_i)=V(x_{i+1})+V(x_i) \tag{6}$$

Figure 5 shows the pulse height spectra measured at about 3.8 MeV electron beams.

4. Bremsstrahlung Spectra

4-1 Energy to Pulse Height Calibration

In a plastic scintillator Compton scattering becomes important at a few MeV. Then the flat part of spectrum, Compton continuum is predominantly produced by Compton electrons, owing to the escape of recoil γ-rays. Other reasons for the part are partly owing to the escape of secondary electrons and to bremsstrahlung produced by them. As known, the energy distribution of the Compton electrons is given by

$$\left.\begin{aligned}\frac{d\sigma(\varepsilon)}{d\varepsilon}&=\frac{\sigma_0}{\gamma^2}\left[2+\frac{\varepsilon\{\varepsilon(\gamma+1)^2-\gamma(\varepsilon^2+2\gamma)\}}{\gamma^2(\gamma-\varepsilon)^2}\right]; \quad 0\leq\varepsilon\leq\frac{2\gamma^2}{2\gamma+1}\\ &=0 \qquad\qquad\qquad\qquad\qquad\qquad ; \text{ others}\end{aligned}\right\} \tag{7}$$

where $\sigma_0=2.495\times10^{-25}$ cm^2, γ is the energy of γ-rays and ε that of the Compton electron, both values are given in m_0c^2 units.

In order to determine the energy to pulse height calibration curve for the plastic phosphor, the well-known Compton edges of monoenergetic γ-rays are used. The Compton edge ε_c (m_0c unit) is given by

$$\varepsilon_c=\frac{2\gamma}{1+2\gamma}\cong\gamma-0.5. \tag{8}$$

At low energy (below about 2 MeV), the Compton edge peak may not be observed for a small crystal practically. In this case, the curve can be graphically writtern from several γ-rays sources of the known Compton edge energy as shown in figures 6 and 11. On the pulse height spectrum the axis of Compton edge energy are provided as a vertical line. At the Compton edge energy of each reference isotope, the segment of the horizontal line having a length corresponding to the range of height is drawn where the embeded edge is expected. Provided that a line cuts across all of the horizontal lines of several edges, it may be regarded as the energy to pulse height calibration curve. In this experiment the calibration curve is expressed as

$$h=(210\pm10)E \tag{9}$$

where E is the Compton electron energy in MeV and h is the pulse height in mV, and shown in figure 6.

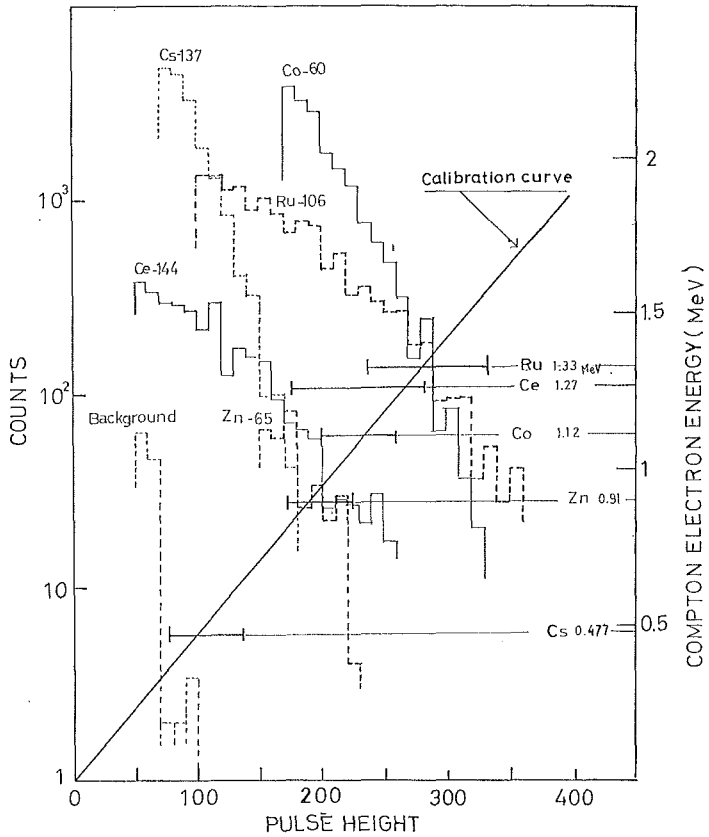

Fig. 6. Compton electron energy to pulse height calibration curve

4-2 Response Function

In the plastic scintillator, Compton scattering is predominant at several MeV. The response function of it may be have the form[3]

$$R(\gamma, h) = \frac{\eta(\gamma)\,\sigma_0}{\sqrt{2\pi}\,\gamma^2}\int_0^{\frac{2\gamma^2}{2\gamma+1}} \frac{e^{\frac{(h-\varepsilon)^2}{2V(\varepsilon)}}}{\sqrt{V(\varepsilon)}}\left\{2+\frac{\varepsilon(\gamma^2+1)-\gamma(\varepsilon^2+2\gamma)}{\gamma^2(\gamma-\varepsilon)^2}\right\}d\varepsilon \qquad (10)$$

where $V(\varepsilon)$ is the variance of the line shape assumed by Gaussian distribution. The efficiency of the Compton effect $\eta(\gamma)$ is expressed as

$$\eta(\gamma) = 1-e^{-\mu(\gamma)L} \qquad (11)$$

in the case of good collimation, where $\mu(\gamma)$ is the linear absorption coefficient of photons, and L is the thickness of the scintillator (Fig. 9). In order to determine the line shape, we used the method of Keszthelyi et al. They defined the energy difference between 3/4 and 1/4 value of the height on the high energy side of the Compton peak as a relative slope S (Fig. 7). The relation between the slope and the variance is

$$S = 0.915\sqrt{V}\,. \qquad (12)$$

The energy dependence of the relative slope is shown in figure 8 and expressed as

$$S/E = 0.15/\sqrt{E} \tag{13}$$

where E is the Compton electron energy in MeV.

The response functions (10) numerically integrated by the Simpson method are shown in figure 10 and are compared with experimental pulse height distri-

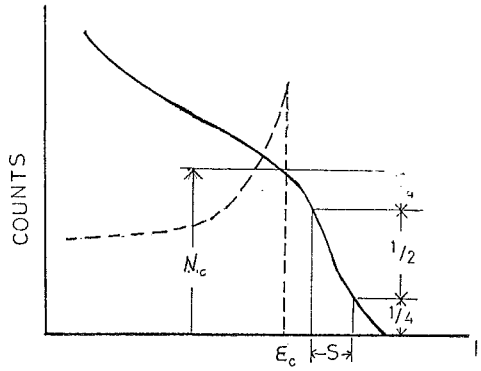

Fig. 7. Relative slope of Compton peak

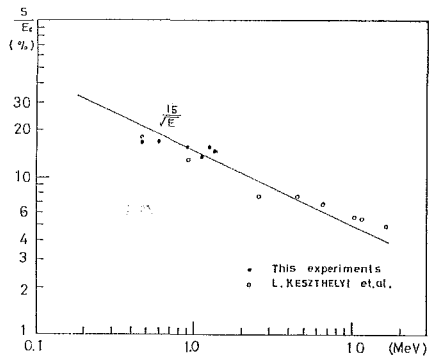

Fig. 8. The energy dependence of the relative slope.

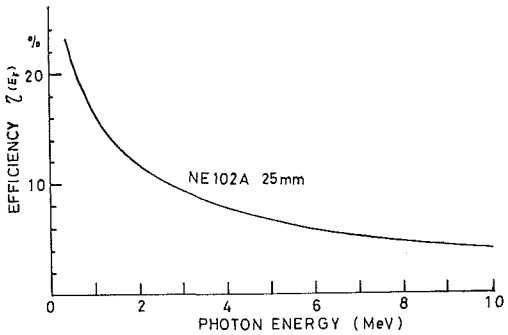

Fig. 9. Efficiency curve of the plastic scintillator (NE 102A, 25 mm-thickness)

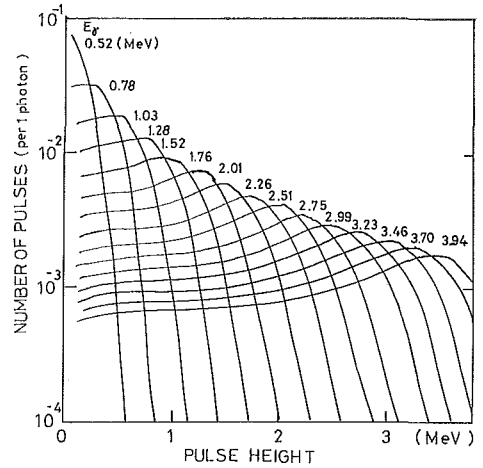

Fig. 10. The response functions numerically intergated

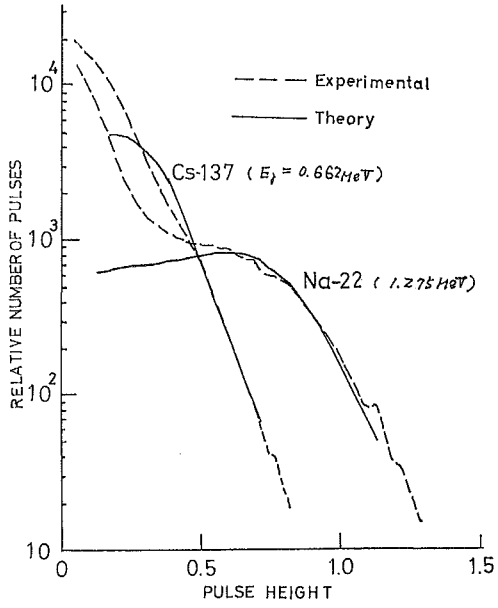

Fig. 11. Experimental pulse height distributions of γ-rays from ^{137}Cs and ^{22}Na

butions of the γ-rays from ^{137}Cs and ^{22}Na in figure 11. Our calculated function of ^{22}Na does not include its annihilation γ-rays. Expect for this they agree fairly well with the results of our experiments and our calculated results also agree with Keszthelyi's experiment of 6.14 γ-rays[3].

4-3 Unfolding Techniques

Pell-off methods, iterative techniques, direct inversions and differential methods were tried to obtain incident photon spectra. Systematic reviews of these methods except for the differental method are taken in the reference 5). The differential method is usually used for the determination of neutron energy spectra by proton recoil techniques. In rough approximation, the response function may be repressed by a rectangular distribution extending from zero energy up to the Compton edge. The height of such a rectangle would be assumed equal to

$$C(\gamma, \varepsilon) = \frac{2\gamma+1}{2\gamma^2}\left[1-u\left(\varepsilon-\frac{2\gamma^2}{2\gamma+1}\right)\right] \tag{14}$$

where $u(x-x_0)$ is the unit step function jumping at x_0. The pulse height distribution of a photon energy $\phi(\gamma)$ is represented by

$$R(h)=\int_0^\infty \frac{2\gamma+1}{2\gamma^2}\left[1-u\left(h-\frac{2\gamma^2}{2\gamma+1}\right)\right]\eta(\gamma)\,\phi(\gamma)\,d\gamma\,. \tag{15}$$

If we differentiate with respect to h and put $h=2\gamma^2/(2\gamma+1)$, we have

$$\frac{dR(h)}{dh}=\left[\frac{(2\gamma+1)^3}{8\gamma^3(\gamma+1)}\,\eta(\gamma)\,\phi(\gamma)\right]_{\gamma=h+\sqrt{h^2+2h}}\,. \tag{16}$$

Specially for mono-energetic photons (energy γ_0), it reduces

$$\frac{dR(h)}{dh}\cong-\frac{2\gamma_0+1}{\gamma_0^2}\,\eta(\gamma_0)\,\delta\left(h-\frac{2\gamma_0^2}{2\gamma_0+1}\right) \tag{16 a}$$

and at higher energies, $\gamma>1$

$$\frac{dR(h)}{dh}\cong\left[\frac{1}{\gamma}\,\eta(\gamma)\,\phi(\gamma)\right]_{\gamma=h} \tag{16 b}$$

or

$$\phi(\gamma)\cong\left[\frac{dR(h)}{dh}\cdot h\Big/\eta(h)\right]_{h=\gamma}\,. \tag{16 c}$$

From equations (16), (16 a) and (16 c), the rough photon energy spectra can be obtained.

In peel-off methods, the response matrix must be triangular, because the contribution associated with each energy component is subtracted in succession starting with component of the highest energy from the observed pulse-height distribution. The response matrix calculated from equation (10) transforms to the triangular which contains elements only below the principal diagonal, omitting the above diagonal elements which have only small values.

In other methods of unfolding we used the response matrix shown in figure

10, which is numerically calculated from equation (10).

The resultant spectra are shown in figure 11 with a spectrum from thin targets calculated from Koch and Motz's formula 2 BN[10]. The result of the iterative method is not shown in the figure because the energy spectra at higher energy regions oscillate in direct inversion fashion as shown in figure 11. Except for this region the data shown in figure 12 are consistent with the general bremsstrahlung characteristics.

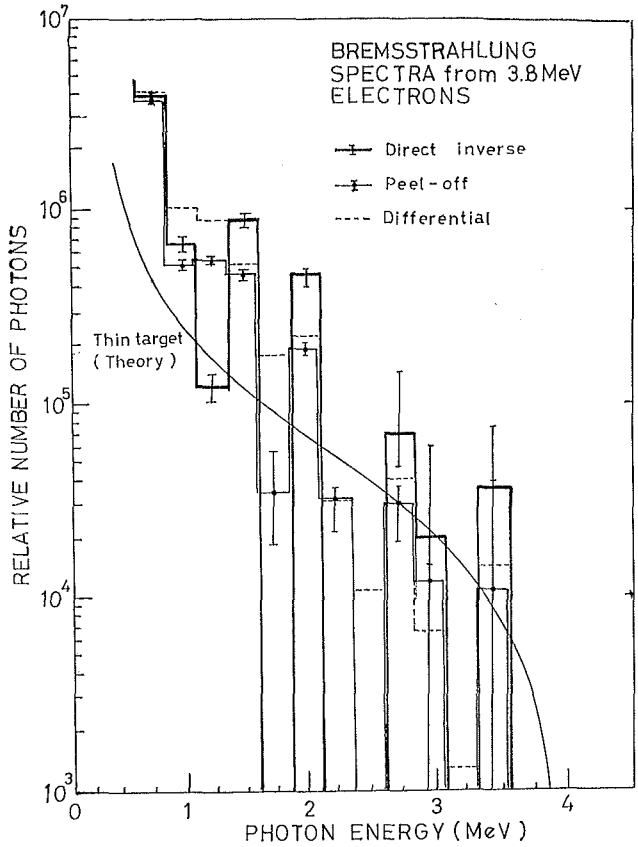

Fig. 12. Bremsstrahlung spectra from thick target bombarded by 3.8 MeV electrons

5. Discussion

The experimental outline here shows that it is possible to measure linac bremsstrahlung spectra readily using simple devices. However it is also found that a plastic scintillator gives only a rough estimation of the final spectra. The statistical errors of the measurement to the final representation are propagated. The noise contribution to the solution vector along the base vector is proportional to the inverse of the smallest eigen-value of the response matrix. On bremsstrahlung spectra, the count rate at high energies decreases exponentially.

Therefore the smallest eigen-value is extremely small in comparison with larger ones. Then the larger noise amplification gives rise to a meaningless distribution at the high energy part. Direct inversion and iterative methods seem to directly reflect this noise amplification, so that the oscillational solutions are obtained. On the other hand, although the differential and peel-off methods are roughly estimated, they give handy unfolding. If a fast single channel analyzer and a computer on line are introduced, it is very convenient to control of the fact discriminater level, to set the time constant of the integrator and to use of unfolding automatically.

In the use of above 10 MeV electron beams, adding to the complex response of plastic scintillator for photon interaction, fast neutrons and photons discrimination problem rises to the spectrum measurement. The pulse shape discrimination technique (PSA) is useful for this purpose.

Acknowledgement

The authors wish to thank Mr. A. Homma of our laboratory for his cooperation in the experiment. This investigation was supported in part by the grant in aid for scientific research of the Ministry of Education.

References

1) McGuire, R. L., Sandifer, C. W.: IEEE Trans. Nucl. Sci. NS-13 [1], (1961), p. 315.
2) Narita, M., Ozawa, Y.: J. Nucl. Sci. Tech., **10** (1973), p. 739.
3) Keszthelyi, L. et al.: Nucl. Instr., Meth., **10** (1961), p. 193.
4) Müller, R., Maeder, D.: Single Crystal Spectroscopy, Chap. VII in Scintillation Spectroscopy of Gamma Radiation, Vol. 1, Gorden and Breach, London (1967), p. 267.
5) Monahan, J. E.: Unfolding Measured Distribution, Chap. VIII in reference (4), p. 371.
6) Ozawa, Y., Narita, M., Kaji, I.: J. At. Energy Soc. Japan, **5** (1963), p. 190.
7) Narita, M., Ozawa, Y.: Japan J. Appl. Phys., **7** (1968), p. 422.
8) Narita, M., Tanida, H., Ozawa, Y.: J. At. Energy Soc. Japan, **13** (1971), p. 248.
9) Narita, M. et al.: Oyo butsuri, **32** (1963), p. 363.
Translation: NSJ-tr-4 (JAERI, Japan 1966).
10) Koch, H. W., Motz, J. W.: Rev. Mod. Phys., **31** (1959), p. 4.